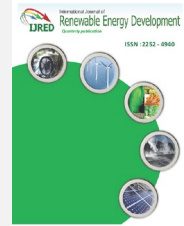




Contents list available at IJRED website

Int. Journal of Renewable Energy Development (IJRED)

Journal homepage: <https://ijred.undip.ac.id>



Research Article

Numerical Analysis of Velocity Magnitude on Wave Energy Converter System in Perforated Breakwater

Oki Setyandito^{1*}, Nizam², Andrew John Pierre¹, Gede Dharma Suputra²,
Yureana Wijayanti¹, Martin Anda³

¹Department of Civil Engineering, Faculty of Engineering, University of Bina Nusantara, Jakarta, Indonesia.

²Department of Civil and Environmental Engineering, Gadjah Mada University, Yogyakarta, Indonesia

³Environmental Engineering Program, Murdoch University, Western Australia

Abstract. Waves are an alternative energy source that can be used for electricity generation. Wave Energy Converter (WEC) system in perforated breakwater is potentially applicable WEC system for coastal area. The magnitude of wave energy generated is determined by the volume of sea water inside the perforated breakwater. This volumetric flow rate is calculated using the flow velocity at perforated holes on the structure slope. Therefore, this research aims to study the velocity magnitude by analyzing the interrelation among wave steepness, wave run-up and relative velocity. The method used consists of applying numeric 3D flow model in the perforated structure of the breakwater with the variation of wave height, wave period and structure slope. The result shows that, the steeper the structure, the bigger is the relative run up (Ru/H). The higher the relative run up, the higher are the relative run-up velocities (V/V_{ru}). As the velocity increase, the volumetric flow rate inside perforated breakwater will be higher, which leads to higher wave energy. Hence, it can be concluded that the higher the velocities (V/V_{ru}), the higher is the wave energy generated.

Keywords: Wave run-up, flow velocity, perforated structure, wave energy

Article History: Received: 4th June 2021; Revised: 18th August 2021; Accepted: 29th August 2021; Available online: 5th Sept 2021

How to Cite This Article: Setyandito, O., Nizam, N., Pierre, A.J., Suputra, G.D., Wijayanti, Y., Anda, M. (2022) Numerical Analysis of Velocity Magnitude on Wave Energy Converter System in Perforated Breakwater. *Int. Journal of Renewable Energy Development*, 11(1), 27-33
<https://doi.org/10.14710/ijred.2022.38535>

1. Introduction

One of the abundant renewable energy sources available on earth is ocean wave energy. More than seventy percent of the earth's surface are oceans. In last two decades, wave energy has been widely developed and regarded as a renewable energy resource with high potential (Falcão, 2010). The increase of human population and technology had caused higher consumption of electrical power all over the world (Malla *et al.*, 2020). Ocean wave energy is an alternative energy source that is very clean, environmentally friendly, always exists and is renewable, predictable, and has developed into a suitable potential alternative energy source to compete with current non-renewable energy sources (Martins *et al.*, 2005).

Utilizing waves as a source of renewable energy offers significant focal points over other methods of energy generation such as solar and wind. Sea waves offer the highest energy density as it can travel large distances with little energy loss. By utilizing sea waves, the yielded power density is 2 - 3 kW/m² compared to solar with power intensity only up to 0.2 kW/m² or wind with power intensity up to 0.6 kW/m² (Mwasilu *et al.*, 2019). The minimum values of wave height, tidal range, current and wind speed that make wave generation a profitable

initiative are 1.6 m (Cruz, 2008), 2.0 m (Charlier and Finkl, 2009), 0.5 m/s (Yuningsih *et al.*, 2010) and 4.0 m/s (Khaligh and Onar, 2013), respectively.

Indonesia is an archipelago with sufficient wave energy potential (Puspita *et al.*, 2020). With the increasing demand for energy today, Indonesia should be able to use its oceans as an alternative energy source, at a time when fossil fuels and non-renewable oil are running low on supplies (Aminuddin, 2018).

Various kinds of research in wave energy converter (WEC) systems have been intensively developed (El Marjani *et al.*, 2008; Elbisy, 2015; Folley *et al.*, 2006; Tseng *et al.*, 2000). Integration of WEC systems in breakwaters is considered as the most applicable WEC systems for port and coastal areas compared to other WEC systems installation (Cascajo, 2019). Perforated breakwaters are one type of perforated structures which have been successfully applied on sloping beaches (Elbisy, 2015). The energy generated in perforated breakwater is determined by the magnitude of sea water volume inside the structure. This sea water discharge is a function of velocity at holes on the perforated structure slope. By understanding the interrelation among velocity, wave run-up, and wave steepness, we could determine the velocity magnitude.

* Corresponding author: osetyanditol@binus.edu

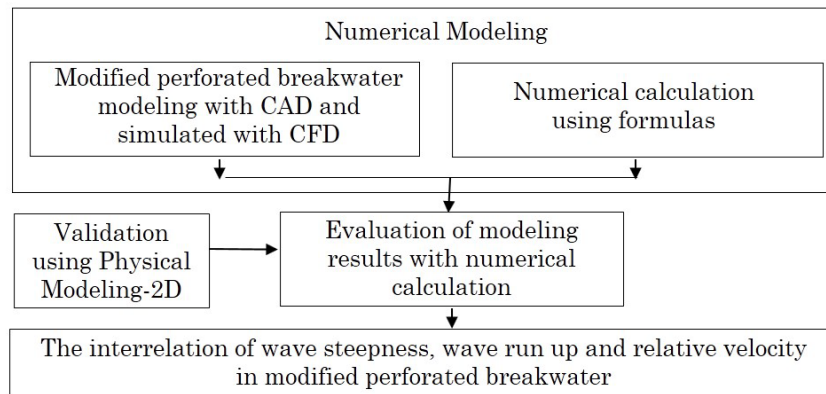


Fig. 1 Flow chart of Research Methodology

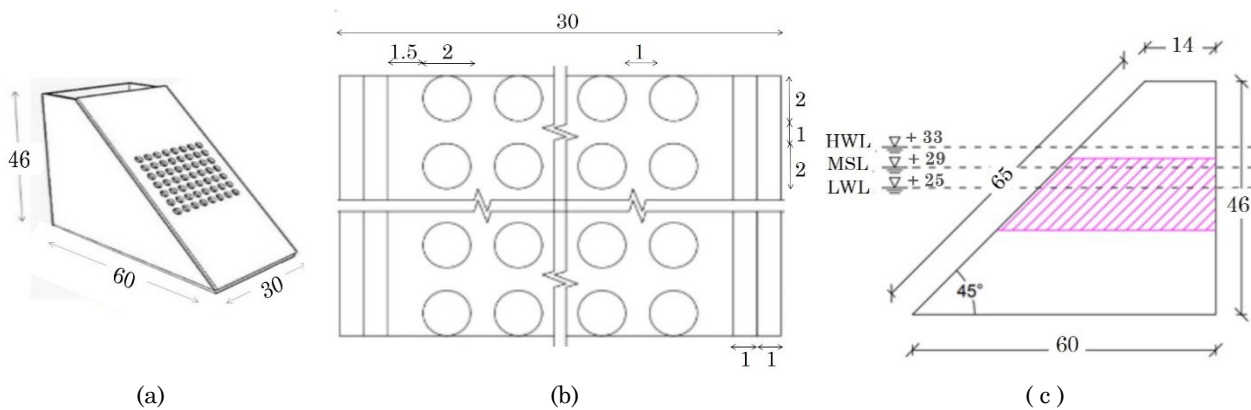


Fig. 2 Modified perforated breakwater (in cm): a. dimension and b. perforated holes layout, c. water depth variation

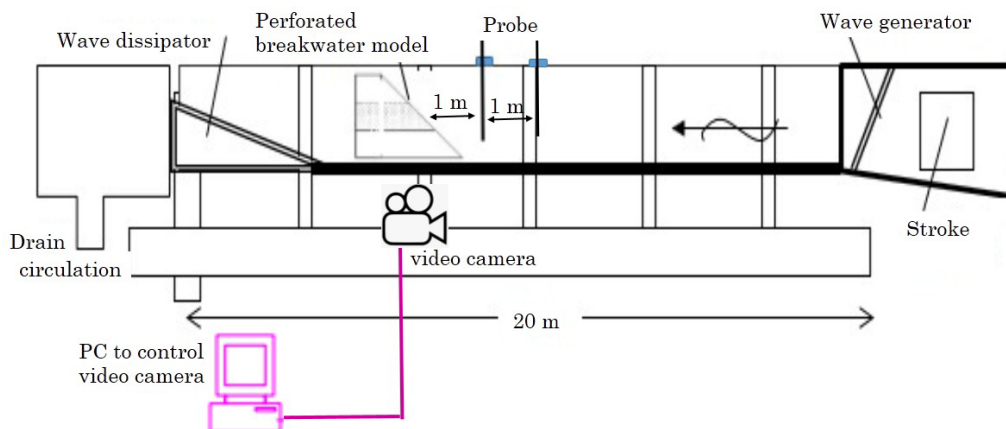


Fig. 3 Experimental setup of physical modeling 2D

Therefore, in this study, a preliminary experiment was performed to investigate the relationship among velocity, wave run-up and wave steepness in perforated breakwaters with the variation of structure slope.

2. Methodology

The flow velocity of wave through a perforated breakwater due to run-up waves will be modeled (Fig. 1). After the

model geometry of a perforated breakwater slope has been created, numerical modeling was carried out using one of the Computer Fluid Dynamic (CFD) programs, namely FLOW-3D (Abdullah *et al.*, 2017; Setyandito *et al.*, 2020).

Various conditions determine the dimensions of the modified perforated breakwater. The modified perforated breakwater modelling measure is based on the HWL (High Water Level), MSL (Mean Sea Level) and LWL (Low Water Level) values that occur at model variation.

According to López *et al.* (2015), the capture factor measures the efficiency of the oscillating water column (OWC) chamber by comparing the pneumatic power to the incident wave power. The tidal level affects the capture factor, which depends on the damping value—it increases with small and intermediate damping but falls with large damping. Tests in regular or monochromatic waves are mainly conducted. A slope angle of 45° to 75° for the modified perforated breakwater is used to increase the amount of dynamic pressure in the modified perforated breakwater space (Binumul *et al.*, 2015).

The modified perforated breakwater model was tested in the computer of BINUS University laboratory. The modified perforated breakwater model and its dimensions are demonstrated in Fig. 2a. The diameter of the holes was 2 cm (Fig. 2b) and the porosity was 0.09. Porosity is the area of total hole space in a model unit (56 holes) divided by the surface slope area (30 cm x 65 cm). The water depth variations at HWL, MSL and LWL are 33 cm, 29 cm, and 25 cm, respectively (Fig. 2c). The initial fluid elevation was set at 0.25 m, and the wave was generated at the inlet of the flume using Stokes (Binumul *et al.*, 2015). Simulations were conducted with wave height of 0.15 m, mean fluid depth 0.25 m, wave period 8 s, current velocity (x-direction) 0,7528 m/sec. The numerical modelling was run using an intel i7 16 processors computer, with a 240 s finish time of running. Physical modeling was using the wave flume with length, width and height of 20 m, 1 m and 1.5 m, respectively (Fig 3). The probe utilized to measure the water particle velocity in front of the perforated breakwater. A video camera installed to record the water particle velocity inside breakwater.

In this experiment, the air compressibility is negligible because the model scale utilized is small (Zhang *et al.*, 2012). As such, the study only simulated water as the fluid inside the modified perforated breakwater space with applying FLOW-3D CFD 3D model. FLOW-3D could model the complex drag phenomena and utilize the proper fluid volume method to trace the fluid interface (Mampaey & Xu, 1995). The 3 (three) dimensional representation of mass continuity and momentum are shown by equations (1) and (2), respectively, below:

$$V_F \frac{\partial p}{\partial t} + \frac{\partial}{\partial x_i} (\rho u_i A_i) = 0, \tag{1}$$

$$\frac{\partial \rho u_i}{\partial t} + \frac{1}{V_F} \frac{\partial (\rho u_i u_j A_j)}{\partial x_j} = -\frac{\partial p}{\partial x_i} + \rho g_i + \frac{1}{V_F} \frac{\partial}{\partial x_j} A_j \left[\mu \left(\frac{\partial u_i}{\partial x_j} + \frac{\partial u_j}{\partial x_i} \right) - \rho (u'_i u'_j) \right] = 0 \tag{2}$$

where ρ is density of fluid, g_i is gravity, i and j in subscript as 1, 2, 3 defining the x-, y- and z-directions, x_i and x_j are the cartesian coordinate, u_i and u_j are the averaged velocity components in subscript direction, t is time, p is the averaged pressure, μ is the absolute viscosity of the fluid, V_F is the fractional volume open to the flow, A defines the area for the subscript direction, and lastly the $\rho(u'_i u'_j)$ is the Reynolds stresses term.

Yakhot and Orszag (1992) initially derived the RNG (Renormalization Group) turbulent model based on the k- ϵ turbulent model and improved it by Yakhot *et al.* in Shih *et al.* (1995) with scale expansions for the Reynolds stress and production of dissipation terms. Speziale and Thangam in Siginer (2015) specified that the RNG model could be a turbulence model, both for practical engineering and scientific purposes. Then, both numerical and

physical 3D modeling result are analysed (Shih *et al.*, 1995; Siginer, 2015).

3. Result and Discussion

3.1 Wave Run-up on Breakwaters

The run-up phenomenon on standing waves has been analyzed in various studies (Byeon & Wang, 2002; Cascajo *et al.*, 2019; Hajivalie *et al.*, 2008; Tsai *et al.*, 1999). Saville (1956) and Whalin (1971) recommended the equation (3) and (4), both are equations for wave run-up on slopes of small beach for wave steepness with high values, as follows:

$$\frac{R}{H} = \sqrt{\frac{H}{2\beta}} + \frac{nH}{L} \left(\frac{1}{\tanh\left(\frac{2nd}{L}\right)} \right) \left[1 + \frac{3}{4 \sinh^2\left(\frac{2nd}{L}\right)} - \frac{3}{4 \cosh^2\left(\frac{2nd}{L}\right)} \right] \tag{3}$$

Where L is the wave length and d is the depth of water.

$$\frac{R}{H} = \frac{\tan\theta}{\left(\frac{H_0}{L_0}\right)^{0.4}} \tag{4}$$

Where H_0 is the deep wave height and L_0 is the wave length of deep water.

Hsu *et al.* (2012) recommended an empirical equation (5) and (6) for the estimation of regular wave run-ups on different sloping structures, with plane and impermeable slope. This equation includes two parameters: the Irribarren number ξ and the structure slope $\tan \theta$:

$$\frac{Ru}{H} = \xi, \text{ for } \xi \leq 2 \text{ and } \tan \theta \leq \frac{1}{5} \tag{5}$$

$$\frac{Ru}{H} = 2 \left(\frac{\xi}{2}\right)^{0.04/\tan^2 \theta}, \text{ for } \xi > 2 \text{ and } \tan \theta > \frac{1}{5} \tag{6}$$

In equation (5) and (6), the surf similarity parameter is utilized to accommodate the relative importance of wave breaking on a sloping beach. The independent parameter is the beach slope, which is utilized in the equation to implement the gravitational effect on the wave run-up on a sloping breakwater structure.

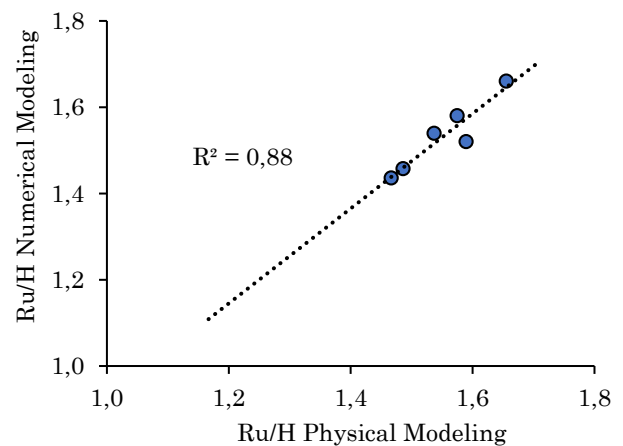


Fig. 4 The relation between numerical and physical modeling of relative wave run-up (Ru/H)

Equation (7) is valid for the Irribarren number ξ beyond the conventional range of $\xi \leq 2$ and for sloping breakwater structures within the range of $1/5 < \tan \theta < 1/2$. According to Meer and Breteler (1990), the run-up velocity becomes:

$$v_{up} / \sqrt{gH} = \sqrt{1/2\pi} \sqrt{(1-z/R_u)} \quad (7)$$

Where R_u is the maximum run-up relative to the sea water level (SWL) and z is the location along the slope, measured in vertical relative to the SWL.

Relative wave run-up from numerical and physical modeling of 45° slope are utilized to validate the simulation (Fig 4).

3.2 Analysis of Experimental Results

The wave tank generated linear waves with a length of wave (λ) of 2 m and wave height of 0.02 m in a water depth of 0.5 m. The size of the dx grids varies from 0.1 m, 0.05 m, 0.025 m, and 0.01 m. Fig. 5 shows that from the different sizes of the grids of $dx = 0.025$ m and $dx = 0.01$ m, that resulting wave height (H) and depth (d) of 0.02 m and 0.5 m, respectively. After that, the relative water depth (d/gT^2) and wave steepness (H/gT^2) were calculated. By using relative water depth and wave steepness value, it is found that the generated wave conforms to the linear wave theory (U.S. Army Corps of Engineers, 2002). However, the grid size of $dx = 0.025$ m is considered adequate to simulate wave interaction with modified perforated breakwater structures.

The 2 (Two) – and 3 (three)-dimensional simulations were then carried out for two different modified perforated breakwater device configurations. Regular waves are defined by their wave height and period. The calculated scale factor compensates for the dimensional scale of these quantities, allowing them to be properly reduced to the model scale. The height of the specified waves is generated by the harmonic oscillation of the wavemaker, which is set to the needed amplitude. Fig. 6 presents a simulation of free surface motion, while the fluid velocity is monitored with a fluid probe (Fig. 7). A regular wave is defined as one in which the waves are in nearly permanent form and where the change in the height of the waves from one cycle to the next occurs within the test duration. The speed and direction of sea currents affect the velocity and path of wave energy. Long and short waves are categorized as tidal and wind waves, and they influence each other in various ways (Neill & Hashemi, 2018).

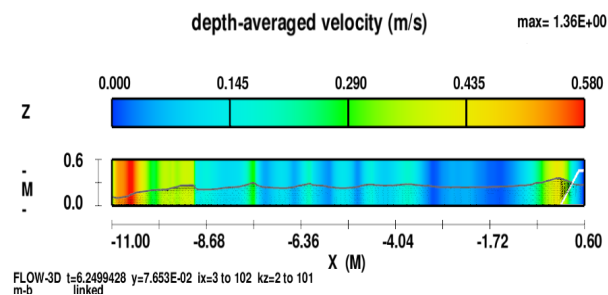


Fig. 5 2D Running Model Variation $d = 0.5$ m in grid sizes of dx are 0.01 m, 0.025 m, 0.05 m, and 0.1

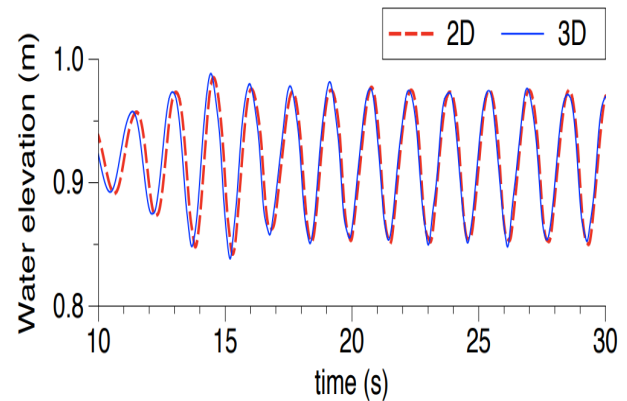


Fig. 6 Comparison of 2D and 3D simulations of free surface motion ($\lambda = 3.56$ m)

The energy conversion rate is equal to the product of velocity and force. The force in linear wave theory is generated by pressure (i.e., $F = pA$), which is related to z . As wave power is a result of pressure and velocity, it can be measured by multiplying these and integrating across depth.

In a symmetrical configuration, as shown in Fig. 8, the front and back walls' immersion depth is the same. As shown in Fig. 8, the back fence protrudes downward in an asymmetrical configuration while the front wall has a definite water depth. The structure dimensions are referred from an experiment conducted by Morris-Thomas *et al.* (2007). In Fig. 8, the velocity formed inside the holes of the modified perforated breakwater increases up to a maximum value of 0.44 m/s. This velocity distribution inside the holes corresponds to velocity variations in the range of 0.45 – 2 m/s within the regular wave field. Fig. 8 also shows that the velocity through holes on the perforated breakwater can be used to supply and generate energy to be converted into an electricity generator. This velocity around perforated slope structures is a function of wave steepness and angle of slope structure.

Although this simulation was conducted in shallow water condition, the wave breaking was prevented to occur by setting the flume boundary condition. The constraint of wave steepness (H/L) < 0.008 for angle of slope structure of 75° .

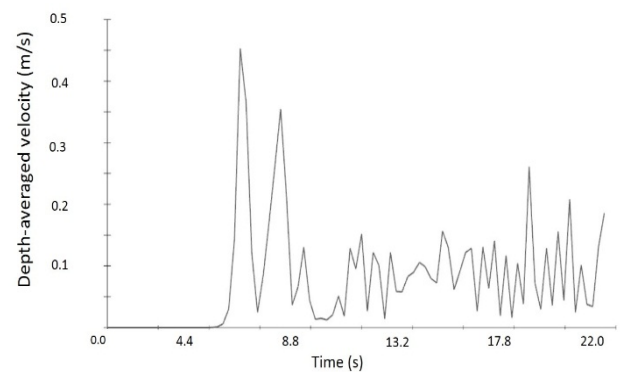


Fig. 7 Fluid velocity magnitude monitored in fluid probe

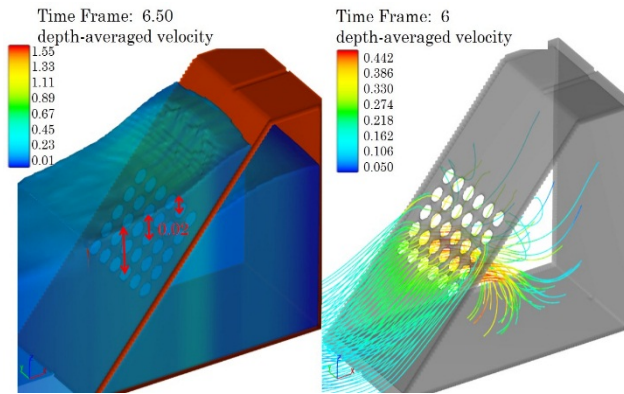


Fig. 8 The velocity at the perforated slope breakwater with average wave height of 0.02 m and λ of 2 m

3.3 Influence of Wave Steepness to the Velocity around Perforated Slope Structures

Wave steepness (H/L) has an inverse relationship with Ru/H (relative wave run-up) at an angle of slope structure within $75^\circ - 45^\circ$ (Fig. 9). The relative wave run-up reduces from 8.63 to 1.75 at wave steepness from 0.002 to 0.054. The following explains why this trend occurs. When the H_o/L_o axis is maximum, so does the wave energy dissipation value, therefore the run-up of wave is decreasing. It is because, as the wave becomes shorter (greater H_o/L_o), then the water particle velocity and acceleration suddenly change. This shift created the turbulence and as a result, the wave energy is dissipated (Elbissy, 2015; Koraim & Rageh, 2013). The energy dissipation can also be caused due to the perforated front of the structure as the H_o/L_o increases (short wave). An increase in H_o/L_o leads to higher flow velocity in the pores. This causes an increase in velocity, which is resulting in more loss of energy. This increase is equal to the square of the flow speed.

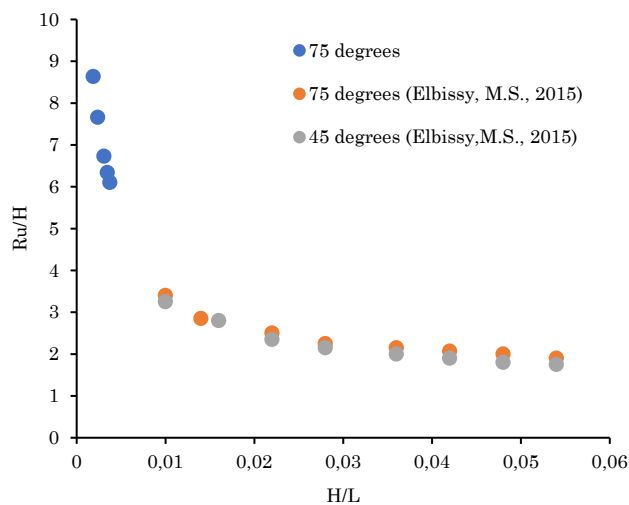


Fig. 9 The relation of wave steepness (H/L) on relative wave run-up (Ru/H)

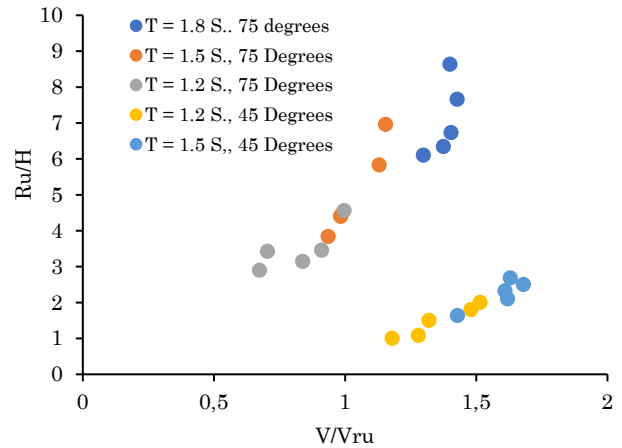


Fig. 10 The relation of relative velocity (V/Vru) on relative wave run-up (Ru/H)

The measured relative run-up velocities (V/Vru) as a function of relative run-up (Ru/H) are shown in Fig. 10 as a function of the angle of slope structure between 45° and 75° . Run-up velocity (Vru) is a flow velocity during wave run up on slope surface. Crucial parameters that determine the relative run-up velocities (V/Vru) are the incident wave steepness and the angle of the structure slope. The fluctuation of wave steepness (H/L) parameter, which is a function of the angle of the structural slope, would influence the relative run-up (Ru/H). The breaker type, breaker criterion, and reflection all influence the relative run-up process. Fig. 10 illustrates that the velocities on a perforated breakwater structure with an angle of slope of 75° and a wave period of 1.2 S., 1.5 S., and 1.8 S., increase from 0.68 m/s to 1.46 m/s. These values refer to the location where transitional wave breaking takes place. The higher the wave period (T), then the higher the run-up velocities (V/Vru). Also, the steeper the structure, the bigger the relative run-up (Ru/H). When the relative run-up velocities (V/Vru) increase, the volumetric flow is also increase, and wave energy generated will likewise increase.

4. Conclusion

The relationship among wave steepness, relative wave and velocity run-up, together with the geometrical characteristic of the perforated structures has been analyzed. The higher the relative wave run up (Ru/H), the lower the wave steepness (H/L) at an angle of slope structure within $75^\circ - 45^\circ$. The higher the wave run up (Ru/H), the higher are the relative velocities (V/Vru). As this velocity increase, the discharge inside perforated breakwater will be higher which lead to higher wave energy. Hence, the higher the relative velocities (V/Vru), the higher the wave energy generated.

Future research is proposed to study the effect of the variation of perforated breakwater performance with variation of wave steepness and the influence of eddy formation in and around the structures, with the purpose of understanding how much potential wave energy can be exploited.

Acknowledgments

This work is supported by Research and Technology Transfer Office, Bina Nusantara University as a part of Bina Nusantara University's International Research Grant. With contract number: No.017/VR.RTT/III/2021.

References

- Abdullah, S. F., Fitriady, A., Hairil, M., & Jusoh, A. (2017). Hydrodynamic performance of cylindrical floating breakwater in waves. *International Journal of Automotive and Mechanical Engineering*, 14, 4715–4729. <https://doi.org/10.15282/ijame.14.4.2017.10.0371>
- Aminuddin, J. (2018). Persamaan Energi untuk Perhitungan dan Pemetaan Area yang Berpotensi untuk Pengembangan Pembangkit Listrik Tenaga Gelombang Laut. *Wave: Jurnal Ilmiah Teknologi Maritim*, 9(1), 9–16. <https://doi.org/10.29122/jurnalwave.v9i1.2647>
- Binumol, S., Rao, S., & Hegde, A. V. (2015). Runup and Rundown Characteristics of an Emerged Seaside Perforated Quarter Circle Breakwater. *Aquatic Procedia*, 4, 234–239. <https://doi.org/10.1016/j.aqpro.2015.02.032>
- Byeon, J., & Wang, Z. Q. (2002). Standing waves with a critical frequency for nonlinear Schrödinger equations. *Archive for Rational Mechanics and Analysis*, 165(4), 295–316. <https://doi.org/10.1007/s00205-002-0225-6>
- Cascajo, R., García, E., Quiles, E., Correcher, A., & Morant, F. (2019). Integration of marine wave energy converters into seaports: A case study in the port of Valencia. *Energies*, 12(5). <https://doi.org/10.3390/en12050787>
- Charlier RH, Finkl CW. (2009). Ocean energy: tide and tidal power. Berlin: Springer; 2009. pp. 38-39.
- Cruz J. (2008) Ocean wave energy: current status and future perspectives. *Heidelberg: Springer*; pp. 220-241.
- El Marjani, A., Castro Ruiz, F., Rodriguez, M. A., & Parra Santos, M. T. (2008). Numerical modelling in wave energy conversion systems. *Energy*, 33(8), 1246–1253. <https://doi.org/10.1016/j.energy.2008.02.018>
- Elbisy, M. S. (2015). Estimation of regular wave run-up on slopes of perforated coastal structures constructed on sloping beaches. *Ocean Engineering*, 109, 60–71. <https://doi.org/10.1016/j.oceaneng.2015.08.059>
- Falcão, A. F. d. O. (2010). Wave energy utilization: A review of the technologies. In *Renewable and Sustainable Energy Reviews* (Vol. 14, Issue 3, pp. 899–918). Pergamon. <https://doi.org/10.1016/j.rser.2009.11.003>
- Folley, M., Curran, R., & Whittaker, T. (2006). Comparison of LIMPET contra-rotating wells turbine with theoretical and model test predictions. *Ocean Engineering*, 33(8–9), 1056–1069. <https://doi.org/10.1016/j.oceaneng.2005.08.001>
- Hajivalie, F., Bakhtiary, A. Y., & Gotoh, H. (2008). *A comparison between standing wave pattern in front of vertical breakwater with horizontal and slope bed*. Conference: ICOPMAS 2008 At: Tehran, Iran. https://www.researchgate.net/publication/262007697_A_comparison_between_standing_wave_pattern_in_front_of_vertical_breakwater_with_horizontal_and_slope_bed
- Hsu, T. W., Liang, S. J., Young, B. D., & Ou, S. H. (2012). Nonlinear run-ups of regular waves on sloping structures. *Natural Hazards and Earth System Science*, 12(12), 3811–3820. <https://doi.org/10.5194/nhess-12-3811-2012>
- Khaligh A, Onar OC. (2010). Energy harvesting: solar, wind, and ocean energy conversion systems. In: Emadi A, editors. *Energy, Power Electronics, and Machines Series*. Florida: CRC Press; pp. 105-111
- Koraim, A. S., & Rageh, O. S. (2013). Hydrodynamic performance of vertical porous structures under regular waves. *China Ocean Engineering*, 27(4), 451–468. <https://doi.org/10.1007/s13344-013-0039-3>
- López, I., Pereiras, B., Castro, F., & Iglesias, G. (2015). Performance of OWC wave energy converters: influence of turbine damping and tidal variability. *International Journal of Energy Research*, 39(4), 472-483. <https://doi.org/10.1002/er.3239>
- Malla, S., Farrok, O., Islam, M. R., & Xu, W. (2020, October 16). Maximization of the Generated Electrical Power of a Superconducting DDLG for Wave Energy Extraction. *2020 IEEE International Conference on Applied Superconductivity and Electromagnetic Devices, ASEM 2020*. <https://doi.org/10.1109/ASEM49065.2020.9276163>
- Mampaey, F., & Xu, Z. A. (1995). *Simulation and experimental validation of mould filling (Book) | OSTI.GOV*. <https://www.osti.gov/biblio/227725>
- Martins, E., Carrilho, L., Neumann, F., Ramos, F. S., Justino, P. A., Gato, L. M. C., & Trigo, L. (2005). *Ceodouro project: overall design of an OWC in the new OPorto break water*.
- Meer, J. W. van der, & Breteler, M. K. (1990). Measurement and Computation of Wave Induced Velocities on a Smooth Slope. *Coastal Engineering Proceedings*, 1(22 SE-Conference Proceedings). <https://doi.org/10.9753/icce.v22.p>
- Morris-Thomas, M. T., Irvin, R. J., & Thiagarajan, K. P. (2007). An investigation into the hydrodynamic efficiency of an oscillating water column. *Journal of Offshore Mechanics and Arctic Engineering*, 129(4), 273–278. <https://doi.org/10.1115/1.2426992>
- Mwasilu, F. and Jung, J.-W. (2019), Potential for power generation from ocean wave renewable energy source: a comprehensive review on state-of-the-art technology and future prospects. *IET Renewable Power Generation*, 13: 363-375. <https://doi.org/10.1049/iet-rpg.2018.5456>
- Neill, S. P., & Hashemi, M. R. (2018). Fundamentals of ocean renewable energy: Generating electricity from the sea. In *Fundamentals of Ocean Renewable Energy: Generating Electricity from the Sea*. Elsevier. <https://doi.org/10.1016/C2016-0-00230-9>
- Puspita, A. D., Pallu, M. S., Thaha, M. A., & Maricar, F. (2020). *The Effect of Wave Deformation on Overtopping Discharge in Wave Energy Converter (OWEC)-breakwater*. <https://medwelljournals.com/abstract/?doi=jeasci.2020.2058.2064>
- Saville, T. (1956). Wave Run-Up On Shore Structures. *Journal of the Waterways and Harbors Division*, 82(2), 925–1. <https://doi.org/10.1061/jwheau.0000017>
- Setyandito, O., Alexander Michael, R. D., Juliastuti, Andrew, J. P., & Wijayanti, Y. (2020). The effect of bridge abutment shape variation toward flow velocity characteristic. *IOP Conference Series: Earth and Environmental Science*, 426(1), 012035. <https://doi.org/10.1088/1755-1315/426/1/012035>
- Shih, T. H., Zhu, J., & Lumley, J. L. (1995). A new Reynolds stress algebraic equation model. *Computer Methods in Applied Mechanics and Engineering*, 125(1–4), 287–302. [https://doi.org/10.1016/0045-7825\(95\)00796-4](https://doi.org/10.1016/0045-7825(95)00796-4)
- Siginer, D. A. (2015). Developments in the flow of complex fluids in tubes. In *Developments in the Flow of Complex Fluids in Tubes*. Springer International Publishing. <https://doi.org/10.1007/978-3-319-02426-4>
- Tsai, C.-P., Lee, T.-L., & Yeh, P.-H. (1999). Forces On Breakwaters By Standing Waves With Water Overtopping. *International Journal of Offshore and Polar Engineering*, 9(03).
- Tseng, R. S., Wu, R. H., & Huang, C. C. (2000). Model study of a shoreline wave-power system. *Ocean Engineering*, 27(8), 801–821. [https://doi.org/10.1016/S0029-8018\(99\)00028-1](https://doi.org/10.1016/S0029-8018(99)00028-1)
- U S Army Corps Of Engineers, N. (2002). *Coastal Engineering Manual*. Coastal Engineering Manual
- Whalin, R. (1971). Run-up and stability of intermediate period water waves at Monterey California. *Dynamic Waves of Civil Engineering*, 265–291.
- Yakhot, V and Orszag, S. A. (1992). Development of turbulence

models for shear flows by a double expansion technique. *Physics of fluids A: Fluid Dynamics* 4, 1510-1520; <https://doi.org/10.1063/1.858424>

Yuningsih A, Sudjono EH, Rachmat B, Lubis S. (2010). Ocean current energy prospect. ESDM, Report. [In Bahasa]

Zhang, Y., Zou, Q. P., & Greaves, D. (2012). Air-water two-phase

flow modelling of hydrodynamic performance of an oscillating water column device. *Renewable Energy*, 41, 159–170. <https://doi.org/10.1016/j.renene.2011.10.011>



© 2022. The Authors. This article is an open access article distributed under the terms and conditions of the Creative Commons Attribution-ShareAlike 4.0 (CC BY-SA) International License (<http://creativecommons.org/licenses/by-sa/4.0/>)